

September 4-7, 2007, Las Vegas, Nevada, USA

DETC2007-34619

## DESIGN OF AN ACTIVE CONTROL ENGINE MOUNT USING A DIRECT DRIVE ELECTRODYNAMIC ACTUATOR

Hyunki Park

Bo-Ha Lee

Chong-Won Lee

Center for Noise and Vibration Control(NOVIC),  
Department of Mechanical Engineering, KAIST,  
Science Town, Daejeon 305-701, South Korea

Email : [hkpark0110@kaist.ac.kr](mailto:hkpark0110@kaist.ac.kr), [look@kaist.ac.kr](mailto:look@kaist.ac.kr), [cwlee@kaist.ac.kr](mailto:cwlee@kaist.ac.kr)

### ABSTRACT

This paper is focused on design of a new active control engine mount (ACM), which is both compact in size and cost effective. The ACM, consisting of an electrodynamic actuator as the active element, flat springs and a sliding ball joint, is different in structure from the previous ACM designs based on the conventional hydraulic engine mount.

Dynamic characteristics of the proposed ACM are extensively investigated before a prototype ACM, which meets the design specifications, is built in the laboratory. For cost effectiveness, a feed-forward control algorithm without a feedback sensor is used for reduction of the transmitted force through the ACM by the engine. The prototype ACM is then harmonic-tested with a rubber testing machine for verification of its control performance as well as adequacy of modeling. Experimental results show that the proposed ACM is capable of reducing the transmitted force by 20 dB up to the frequency range of 60 Hz.

### 1. INTRODUCTION

The role of an engine mount is not only to support engine loads but also to reduce noise and vibration transmitted from engine to chassis. An engine mount should meet two contradictory requirements: it should provide large stiffness and damping for firm support of engine load and small stiffness and damping for effective isolation of the transmitted dynamic force to the chassis.

Because rubber mount or hydraulic mount alone, due to their passive nature, fails in meeting those design requirements simultaneously, active control engine mounts (ACM), which use the rubber and hydraulic mount structure as the basic design but incorporated with an active element, were developed [1,2,3,4].

For safe operation ACM should work, at least, as an ordinary rubber mount under abnormal situations such as actuator malfunctioning, fluid leakage and power disconnection. Solid rubber mount, normally consisting of an elastic element with no significant damping, can be reasonably well described by a three-dimensional spring element. Main rubber mount supports the engine load along the transverse as well as vertical directions.

ACM, which is normally equipped with a single actuator, is capable of generating force only along a specified direction, say, the normal direction. ACM then should be able to function properly, while it absorbs the transverse loadings from the engine. The conventional ACM based on hydraulic engine mounts endure such transverse forces from the engine due to the indirect transmission mechanism of the actuator force through fluid, requiring a complicated structural design with sealing of fluid

This paper is focused on design of a new ACM, which consists of an electrodynamic actuator, flat springs and a ball joint, as well as evaluation of its isolation performance. The ACM is not based on the conventional hydraulic mount and yet it is capable of absorbing the transverse engine loads.

### NOMENCLATURE

$A_g$	: Area of gap
$A_m$	: Area of magnet
$F_{active}$	: Active force of electromagnetic actuator
$F_1, F_2$	: Transmitted forces to chassis through engine mount paths
$F_s$	: Magnetic leakage coefficient

$f_s$	: Magnetic resistance coefficient
$I_c$	: Current to coil
$K_r$	: Rubber stiffness coefficient
$L_g$	: Gap length
$L_m$	: Magnet height
$x(t)$	: Engine displacement
$\mu_0$	: Permeability
$(BH)_{\max}$	: Maximum energy product

## 2. Structure Design and Modeling of ACM

Figure 1 shows the structure of the proposed ACM, consisting of the main rubber and an electrodynamic actuator. The main rubber is directly excited by the runner of the actuator. The ball bearing between the runner end and the main rubber unit, whose contact mechanism along the normal direction is maintained by pre-compressed flat springs, absorbs any probable transverse motion between them.

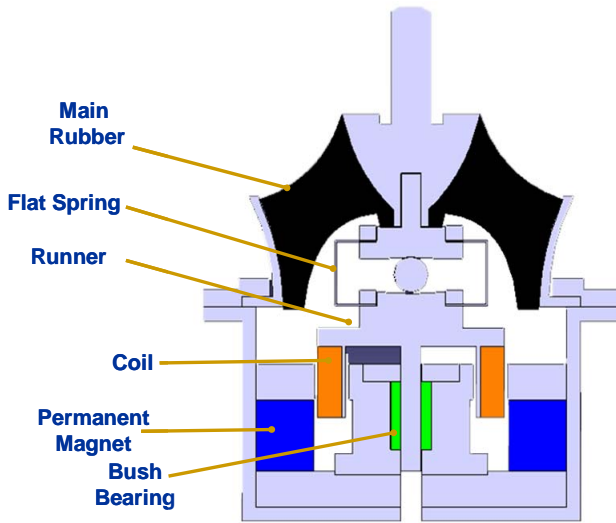


Figure 1. Structure of the active control engine mount

Figure 2 shows of the ACM model, where  $x(t)$  is the engine vibration,  $K_r$  is the stiffness coefficient of the main rubber and  $F_{active}$  is the generated force by the electrodynamic actuator. The total transmitted force  $F_T$  from the engine to the chassis simply becomes, due to absence of fluidic device,

$$F_T = F_1 + F_2 \quad (1)$$

where the forces transmitted through the main rubber and the actuator,  $F_1$  and  $F_2$ , are expressed, respectively, as

$$\begin{aligned} F_1 &= K_r x \\ F_2 &= F_{active} = G_{active} I_c \end{aligned} \quad (2)$$

Here,  $K_r$  is the main rubber stiffness,  $x$  is the relative displacement of the engine to the chassis,  $I_c$  is the control current to the coil and  $G_{active}$  is the electrodynamic constant. Combining equations (1) and (2), we obtain

$$\begin{aligned} F_{active} &= -K_r x + F_T \\ &= -K_r x \quad \text{for } F_T = 0 \end{aligned} \quad (3)$$

The above equation suggests that the actuator force required for complete isolation of the transmitted force from engine to chassis is readily calculated from measurement or estimation of  $x$ .

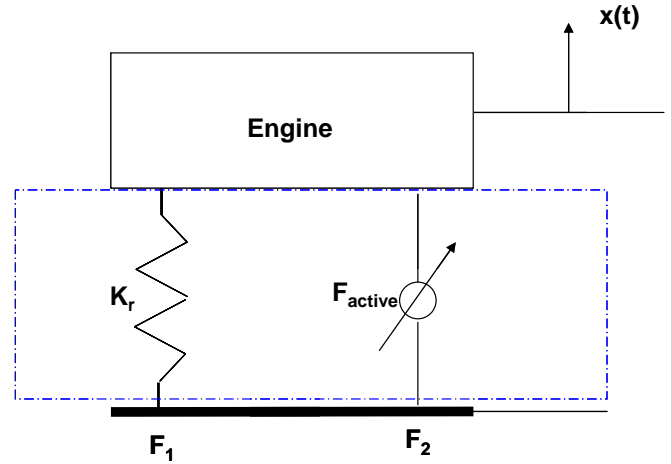


Figure 2. The ACM model

## 3. Design of Electrodynamic Actuator

The electrodynamic actuator should be designed such that it is compact to fit into a specified limited space and yet it generates enough force over the frequency range of interest to cancel the transmitted force from engine to chassis through roll mount. The ACM is developed particularly for the four-cylinder in-line diesel engine of interest, which is a typical passenger vehicle engine. For the engine running from 600 to 3,000 rpm., the maximum dynamic displacement of the roll front and rear mounts is approximately 0.1 mm. It implies that the ACM needs to cancel the transmitted force resulting from the dynamic displacement of 0.1 mm. Considering the main rubber stiffness of 0.4 kN/mm for small displacement, the transmitted force through the main rubber can be calculated to be approximately 40 N. Thus, the required actuator force should be greater than 40 N and its dynamic range of ACM should be from 20 to 100 Hz to cancel the transmitted force to chassis. The ACM runner also should be able to accommodate the static and dynamic engine displacements of 10 mm and  $\pm 1$  mm, respectively. Regarding permanent magnets, the Neodymium 48 series of magnet was used due to its large flux as given in Table 1.

Table 1. Permanent magnet property

Parameter	Value
Remanence, $B_r$	1.37~1.42 Tesla
Coercive force, $H_c$	860~995 $kA/m$
Maximum energy product, $(BH)_{max}$	358~382 $kJ/m^3$
Curie temperature	310~370 $^{\circ}C$

Assuming the ideal magneto- motive force and flux for the gap and magnet, the flux density of gap shown in Fig. 3 is theoretically determined as [5,6,7]

$$B_g = \sqrt{\frac{\mu_0 L_m A_m (BH)_m}{f_s F_s A_g L_g}} \quad (4)$$

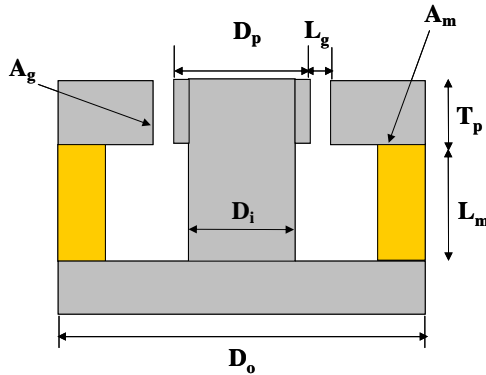


Figure 3. The actuator structure

where the  $A_g$  and  $A_m$  are pole face areas of air gap and permanent magnet,  $L_g$ ,  $L_m$  and  $T_p$  are respectively length of air gap, height of permanent magnet and height of pole face,  $D_p$ ,  $D_i$  and  $D_o$  are center pole diameter, inner pole diameter and outer pole diameter at each. The final design values of the prototype ACM that meets the previous design requirements are listed in Table 2.

Table 2. Design values of the prototype ACM

Parameter	Design value
Electrodynamic force, $F$	42 N
Flux density of gap, $B_g$	0.4 T
Coil length, $l$	56 m
Magnet height, $L_m$	20 mm
Maximum current, $I$	2 A
Coil turns, $N$	410
Height of ACM	160 mm
Diameter of ACM	98 mm

#### 4. Flat Spring & Ball Bearing

Four flat springs of total pre-load of 200 N were used, which was five times as large as the minimum load of 40 N, required to keep the contact between the electrodynamic actuator and the main rubber unit through the ball bearing. It was determined that each flat spring was to be pre-deflected by 22.4 mm to generate the preload of 50 N. The ball bearing, consisting of a ball and the upper and lower concave containers, was designed such that the contact stress be far lower than the allowable yield stress of steel [8].

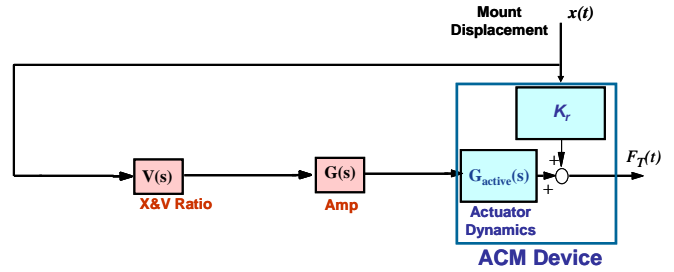


Figure 4. Block diagram for ACM

#### 5. Performance of Engine Mount using Feed-forward Control

A feed forward control algorithm was applied to the active engine mount in order to cancel out the transmitted force from the engine, as shown in Fig. 4. From the measured information of  $K_r$  and  $G_{active}$ , the desired control command for engine vibration displacement was determined as X&V ratio. The electrodynamic actuator generates the control force which is opposite in direction to and of the same magnitude as the transmitted force through the main rubber due to the engine vibration.

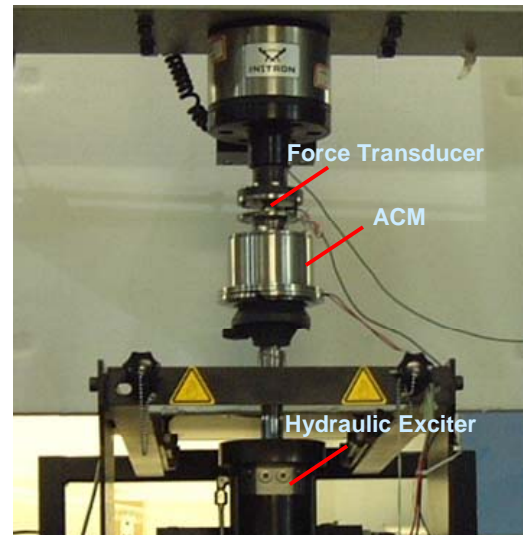


Figure 5. Test setup

Before the testing control performance of the ACM, preliminary harmonic tests for identification of the main rubber

and the actuator dynamics were carried out using a commercial rubber testing machine in the laboratory, which is shown in Fig. 5. Note here that, for convenience of tests, the ACM was mounted upside down throughout the whole tests. For identification of the main rubber, the ACM unit without control was mounted in the testing machine, when the harmonic input displacement was given at the main rubber end, while a force transducer mounted at the fixed end measured the transmitted force. Figures 6 (a) and (b) show the stiffness and loss angle, respectively, of the main rubber as the amplitude and frequency of the main rubber harmonic displacement were varied from 0 to 100 Hz and from 0.1 to 1 mm, respectively. Note that the loss angle is negligibly small and the stiffness of the main rubber is considered to be a real constant over the whole frequency range of interest. The nonlinearity in stiffness of the main rubber with respect to the input level is also considered to be neglected, accounting for the fact that the nominal engine vibration is around 0.1 mm. Such simplistic stiffness of the passive ACM unit, compared with the complicated property of the conventional hydraulic engine mount, is mainly due to absence of fluid in the new design.

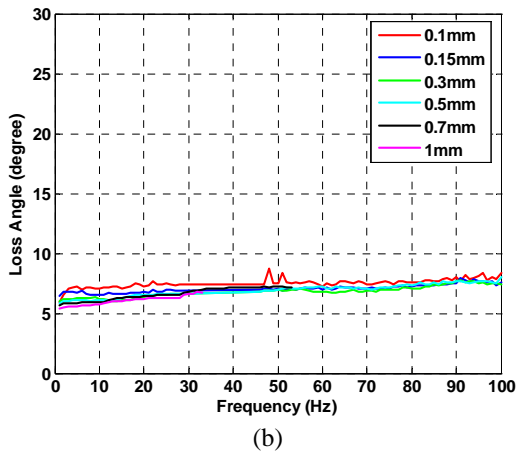
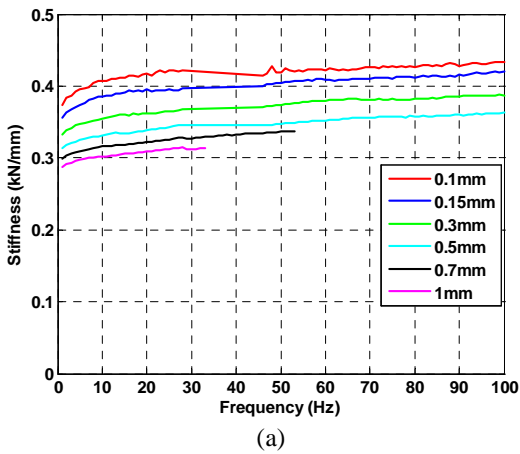


Figure 6. Passive stiffness of ACM: (a) magnitude and (b) phase

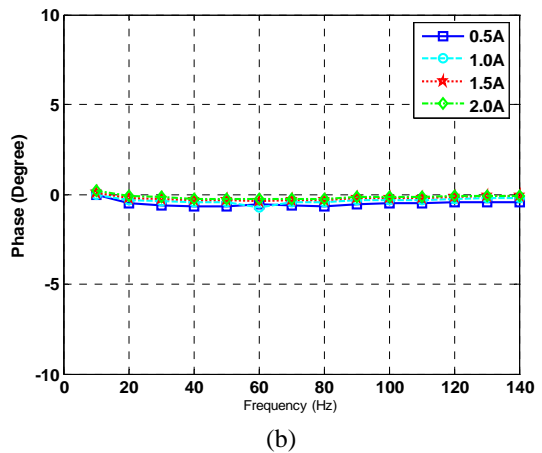
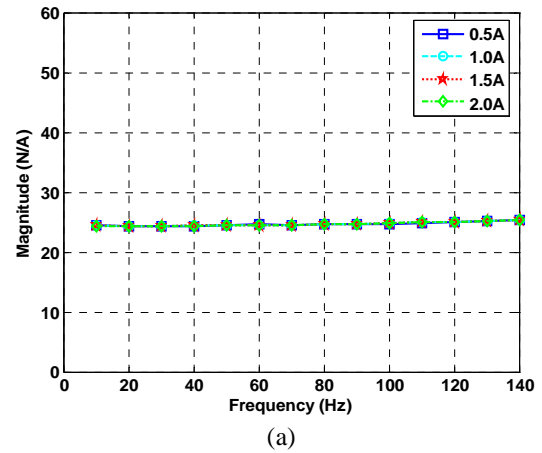


Figure 7. Frequency response function of electrodynamic actuator (input: current, output: force): (a) magnitude and (b) phase

For experimental verification of the actuator dynamics, a harmonic test was performed with the ACM, whose both ends were fixed in the testing machine, as the harmonic input current was fed to the actuator and the force transducer measured the generated force by the actuator. During the tests, the input current level and frequency were varied up to 2 A and 140 Hz, respectively. Figure 7 shows that the actuator force is directly proportional to the input current, irrespective of the variations in frequency and input current level. It can be concluded here that the main rubber model and the actuator dynamics can be well approximated as pure static systems.

After identifying the main rubber and the actuator, the feed forward control algorithm using the dSPACE was applied to the ACM mounted on the testing machine, when the simulated harmonic engine vibration again disturbs the main rubber end and the other end is fixed. During the control tests, the sampling frequency was kept at 10,000 Hz.

The dSPACE calculates the control input to a linear power amplifier, based on the harmonic disturbance information

[9,10]. Typical experimental results are shown in Fig. 8, which simulates the engine idling condition, corresponding to the engine vibration amplitude and frequency of 0.1 mm and 20 Hz, respectively. Note that the main harmonic component has been reduced by over 20 dB after control. The presence of high frequency components remaining even after control is due to the nonlinearities in the system, mainly caused by the friction in the testing machine as well as the runner against the guide.

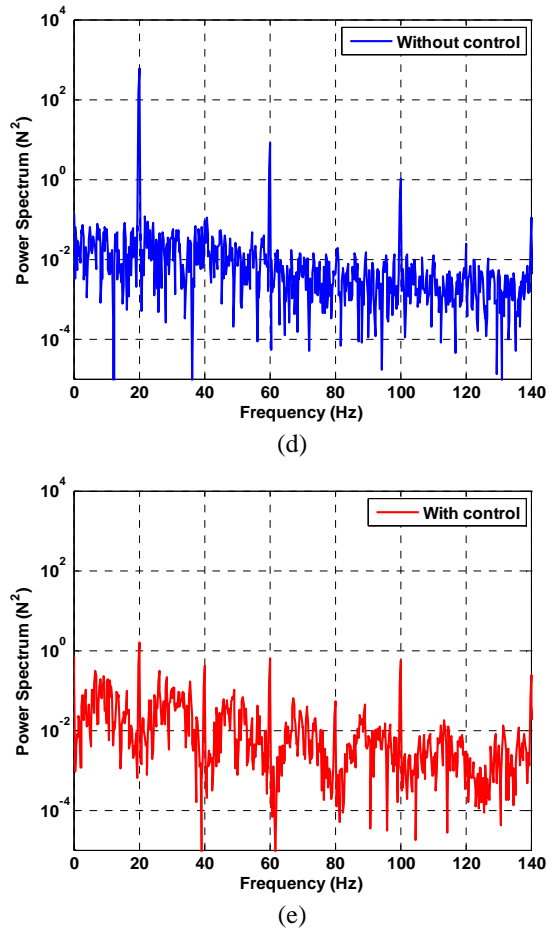
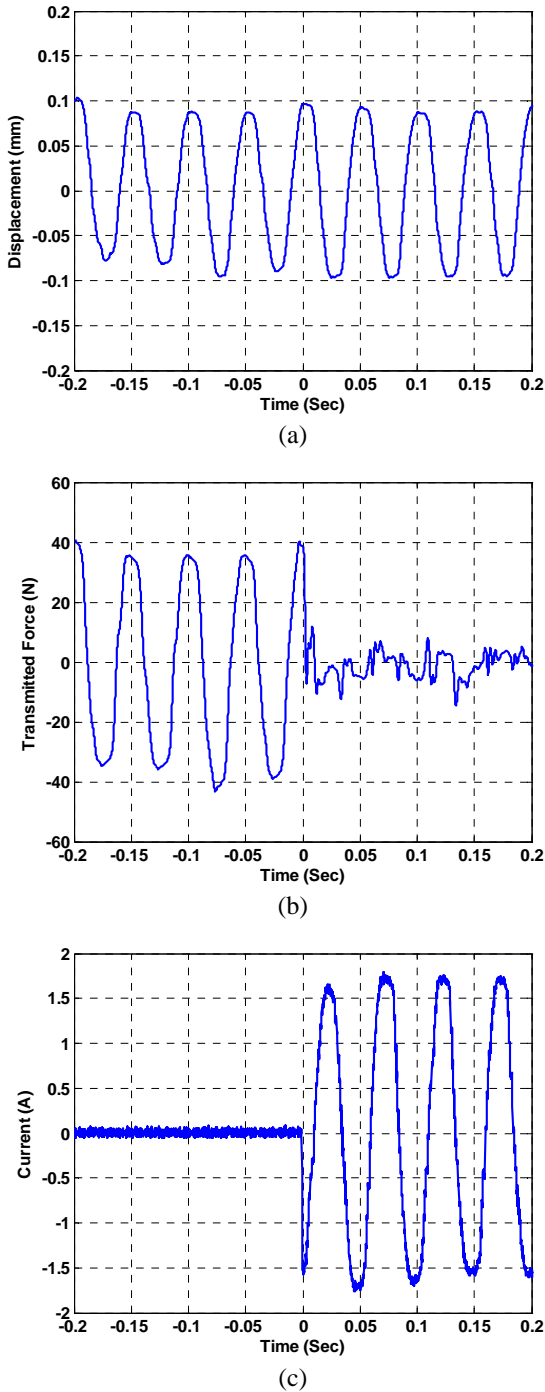


Figure 8. Feed forward control at idle: (a) excitation displacement (b) transmitted force, (c) control current, and power spectra of the transmitted force (d) before and (e) after control

Figure 9 compares the effective stiffnesses of the ACM before and after control, which were calculated using the main harmonic components. The stiffness of the passive ACM is a constant of about 0.4 kN/mm over the frequency range of interest, as stated before. Note from Fig. 9 that the stiffness value of the ACM after implementing control decreased from 0.4 to less than 0.1 kN/mm.

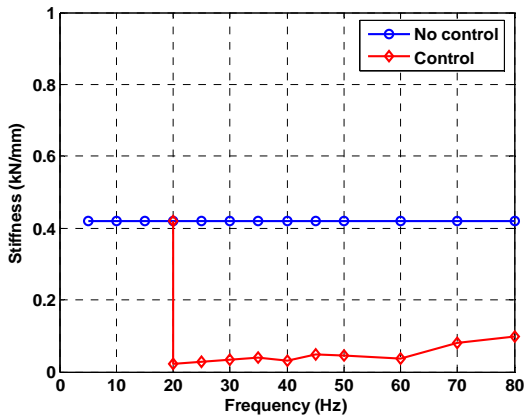


Figure 9. Performance of ACM : effective stiffness

## 6. Conclusion

A new type ACM, which is activated by an electrodynamic actuator, has been developed. It features that the dynamic modeling and control scheme become simple and effective, compared with the ACMs based on the conventional hydraulic engine mount and it does not require a fluid chamber for force transmission. It has been experimentally proven that the ACM with a simple feed-forward control algorithm achieved the vibration isolation efficiency of about 20 dB up to 60 Hz.

## REFERENCES

1. H. Haldenwanger, and P. Klose, "Isolation and Compensation of Vibration by Means of Active Piezo-Ceramic Mount," Proceedings of Advanced Vehicle Control '92, pp.23~27, 1992
2. T. Ushijima and S. Kumakawa, "Active Engine Mount with Piezo-Actuator for Vibration Control," SAE paper 930201, 1993
3. Y. W. Lee and C. W. Lee, "Dynamic Analysis and Control of Active Engine Mount System," Journal of Automotive Engineering, Vol.216, p921-931, 2003
4. H. S. Kim, "Design and Dynamic Analysis of Active Engine Mount using Electro-Dynamic Actuator," MS Thesis, KAIST, 1997
5. H. C. Lee, Design, Manufacture and Performance Test of an Electrodynamic Exciter, MS Thesis, KAIST, 1991
6. M. A. Plonus, "Applied Electromagnetics," McGraw-Hill Book Co., 1987
7. D. Hanselman, Brushless Permanent Magnet Motor Design, The Writers' Collective., 2003
8. W. D. Pilkey, Formulas for Stress, Strain, and Structural Matrices, Wiley, 1994
9. K. Ogata, "Discrete Time Control Systems," Prentice Hall, 1995
10. B. Shahian, Control System Design Using Matlab,